Novel Concepts of Mode Volume and Quality Factor in Research Applications of Photonic Nanocavities and Ring Resonators

EDVCATIO PHYSICORVM
QVO NON ASCENDAM?

ISSN 1870-9095

Kamal Nain Chopra[1] and Shivani Aggarwal[2]
[1]Former Professor Applied Sciences Department, Maharaja Agrasen Institute of Technology, Rohini, GGSIP University, New Delhi - 110086, India;
Former Research Scientist, Photonics Group, Department of Physics, Hauz Khas, New Delhi-110016. India; and
Former Scientist G, Laser Science and Technology Centre, Metcalfe House, Delhi-110054.India;
[2]Applied Sciences Department, Maharaja Agrasen Institute of Technology, Rohini, GGSIP University, New Delhi - 110086, India.

E-mail: kchopra2003@gmail.com

(Received 11 February 2025, accepted 25 May 2025)

Abstract

Novel Concepts of Mode Volume and Quality Factor in Research Applications of Photonic Nano cavities and Ring Resonators have been technically discussed in the present paper. The Localized Modes induced by structural defects have been briefly described. The cases of Air-mode photonic crystal ring resonator and Ultra-compact active hybrid plasmonic resonator have been investigated in detail. Different approaches for modeling the nano cavities have been presented and technically discussed. Some of the important recent experimental breakthroughs in the topic have been qualitatively reviewed by briefly discussing their results. The paper should be really useful for the researchers and designers in this evolving important field.

Keywords: Photonic Nano cavities, Mode volume, Air-mode photonic crystal ring resonator, Ultra-compact active hybrid plasmonic resonator.

Resumen

En este artículo se abordan técnicamente nuevos conceptos de volumen modal y factor de calidad en aplicaciones de investigación de nanocavidades fotónicas y resonadores de anillo. Se describen brevemente los modos localizados inducidos por defectos estructurales. Se investigan en detalle los casos de resonadores de anillo de cristal fotónico en modo aire y resonadores plasmónicos híbridos activos ultracompactos. Se presentan y discuten técnicamente diferentes enfoques para el modelado de las nanocavidades. Se revisan cualitativamente algunos de los avances experimentales recientes más importantes en este tema, analizando brevemente sus resultados. Este artículo resultará de gran utilidad para investigadores y diseñadores en este campo en constante evolución.

Palabras clave: Nanocavidades fotónicas, Volumen modal, Resonador de anillo de cristal fotónico en modo aire, Resonador plasmónico híbrido activo ultracompacto

I. CAPABILITY OF CONFINING AND MANIPULATING PHOTONS AT NANOMETER SCALES

It has now been well established that the capability of confining and manipulating photons at nanometer scales has opened up numerous opportunities in (i) classical and quantum information processing technologies, and (ii) life sciences. Though many research papers have appeared, which demonstrate the submicron light confinement, yet the critical problem lies in the form of challenges in understanding the new device concepts and developing technologies which can operate reliably at nanometer scales. Already, researchers are engaged in making efforts in this direction. In practice, it is found that the large aggregated bandwidths of the optical interconnects are required for the memory and delay components for launching, buffering, and collecting optical signals at the nodes. One of the suggestions has been the use of the two-dimensional coupled nanocavity array structures, having flat electromagnetic bands implying that the frequency variation with the wave vector is minimized in all crystal directions. It is also known now that such structures with reduced rotational symmetries are suitable for strongly controlling the polarization of light. One of the very important uses has been the improvement in the performance of lasers w.r.t. their speed and efficiencies, which can be dramatically enhanced by using nanocavities, because of the fact that the spontaneous emission rate is

enhanced by the modification of vacuum field density in a cavity. Ultra-fast lasers with turn on and turn-off times ~ 1-2 ps. have already been developed, which are able to direct signal modulation speeds >100 GHz, which is even more than an order of magnitude higher than the semiconductor laser speeds.

It is important to note that the speed enhancements of this order have been possible by the ~ 75-fold enhancement of spontaneous emission. Nanocavity lasers with still higher output powers and efficiencies have been achieved by the development of a new device composed of coherently coupled nanocavity laser array. Such devices have been realized by nanofabrication procedures developed for Indium Phosphide and Silicon material systems. It is to be noted that the nanocavities are able to increase sensitivity of bio and chemical sensors. Successful efforts have also been made to integrate the network of such nanocavity detection centers with micro fluidic circuits for high throughput and compact lab-on-a-chip systems. These have also been found useful for detecting the refractive index changes in nanocavities with high sensitivity levels.

II. GUIDING OF LIGHT BY A PHOTONIC CRYSTAL

The band gap in photonic crystals is the forbidden energy range, and hence, wave behaving photons are unable to transmit through the material. Clearly, it is possible to tailor the specific band gap of a structure by defining a pattern with repeating regions i.e. by imitating the periodicity of photonic crystals. This is typically done by forming a structure with holes in a square or hexagonal arrangement, alternating between materials with high and low dielectric constant. The results of Simulation showing how light propagates in photonic crystals, which are available in the literature, have been reproduced below:

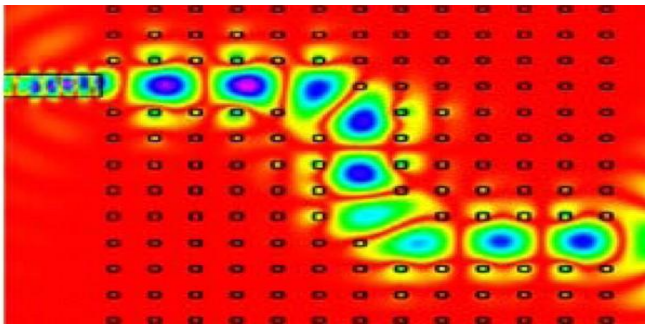

}**FIGURE 1.** Simulation showing how light propagates in a photonic crystal. Figure courtesy http://www.phoenixbv.com.

As illustrated in the above figure, a photonic crystal can be used to guide the light in different directions.

III. MODELING OF PHOTONIC NANOCAVITIES

An important application of photonic crystals is the realization of the optical nanocavities, which are able to trap the light in very small mode volume ($V \approx 2(2/2n)^3$, where n is the refractive index. This small mode volume can lead to significant enhancement of spontaneous emission rates in semiconductor nano-cavities due to the Purcell effect. The spontaneous emission modification factor, also known as the Purcell factor, scales inversely with the cavity mode volume. In nanoscale lasers, enhanced emission together with a reduced number of cavity modes relative to large lasers can have significant effects, especially on sub-threshold behavior and for a long period of time, proportional to the cavity quality factor Q. The underlying physics is simple: The strong light localization in photonic crystal nanocavities results in dramatically increasing the light-matter interaction, and the photon-photon interaction, which leads to their use in a wide range of applications in basic science and engineering. An important strange offshoot is that by combining photonic crystal lattice defects in a linear configuration, we can construct very compact waveguides capable of sharply bending with very low losses; and finally an efficient coupling of these waveguides and cavities on chip, is important for the realization of compact and high bandwidth optical integrated circuits. In addition, the devices can be made in standard electronic materials, in a planar geometry, which can be integrated with electronics to achieve a higher level of functionality.

The studies of the Mode of photonic-crystal-slab single-defect cavity structures have drawn the attention of the researchers for suggesting their use as a good candidate for a high-quality factor (Q) and small-mode volume (V) resonant mode. Ryu et al (1) have optimized the structural parameters to obtain very large of even higher than with small effective of the order of cubic wavelength in material, by using the finite-difference time-domain calculations. It has been suggested by the Fourier-space investigation of resonant modes, that such a high from the hexapole mode is achieved due to the cancellation mechanism related to hexagonally symmetric whispering-gallery-mode distribution and also to the mode delocalization mechanism.

One of the techniques for fabricating Photonic crystal nanocavities is based on modifying one or more holes in a perfectly periodic lattice, which is done by changing the hole size or the refractive index. In fact, a break of this type in the periodicity of the lattice introduces new energy levels within the photonic band gap, in the same way as the creation of energy levels within the semiconductor energy band gap by the addition of the doping atoms in semiconductor crystals. Interestingly, an increase in the hole sizes enhances the energy of the modes held in the slab, and thus pulls up the defect states from the dielectric band into the band gap, the modes created in this being called the acceptor modes. On the other hand, a reduction in the hole sizes decreases the energy of the mode, and hence pulls down the defect states from the air band into the band gap, defect modes of this type being called the donor modes. The Schematic of the point-defect

nanocavity in a 2D photonic crystal (PC) slab is shown below:

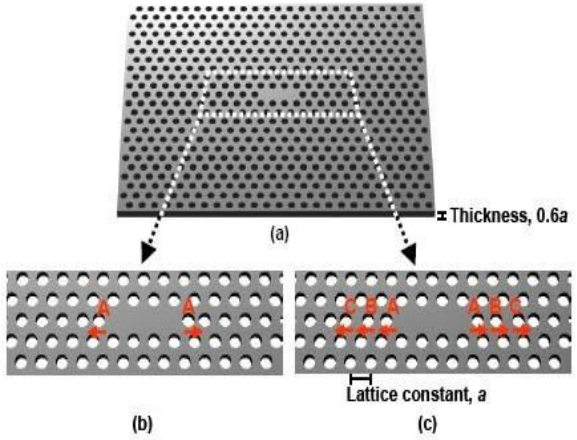

FIGURE 2. Schematic of the point-defect nanocavity in a 2D photonic crystal (PC) slab. The base cavity structure is composed of three missing air holes in a line. The PC structure has a triangular lattice of air holes with lattice constant a. The thickness of the slab and the radius of the air holes are 0.6a and 0.29a, respectively. (b) The designed cavity structure created by displacing two air holes at both edges in order to obtain high-Q factor. (c) The designed cavity structure created by fine-tuning the positions of six air holes near both edges to obtain an even higher Q. Figure courtesy Akahane Yoshihiro, Asano Takashi ,Song Bong-Shik , and Noda Susumu, Fine-tuned high-Q photonic-crystal nanocavity, Optics Express, Vol. 13, Issue 4, pp. 1202-1214, (2005), https://doi.org/10.1364/OPEX.13.001202.

Akahane et al (2) have studied Fine-tuned high-Q photonic-crystal nanocavity. Following the approach supported by them, the Q factors for cavities with a range of air hole displacements at positions A, B and C. can be calculated by applying 3D-FDTD method. The structure is discretized on a 3D mesh and Mur's second-order absorbing-interface condition is applied to the outer surface of the computational domain. For the case of the base 2D-PC slab composed of Silicon with a triangular lattice of air holes having lattice constant a, and for the parameters : slab thickness of 0.6a, air hole radius of 0.29a, slab index of 3.4 and an air clad index of 1; he Q factor of the cavity modes can be expressed as follows:

$$Q \equiv \{\omega_0(t)\}/\{(-dU(t)/\,\mathrm{dt}'\}, \qquad (1)$$

where, ω_0 is the angular frequency of the cavity mode, and $U(t)$ is the total energy stored in the cavity. Eq. (1) can be used to derive the following equation:

$$(t)=[\{U(0)\exp[-(\omega 0t)\}/Q], \qquad (2)$$

and, the magnetic field $H(t)$ can be expressed as follows:

$$\ln[H(t)]=\ln[H(0)]-[\omega 0/(2Q)]t. \qquad (3)$$

As can be seen in Eq. (3), the Q factor can be calculated by measuring the slope of the exponential decay of the magnetic field (or the electric field) of a given cavity mode. Q factor is calculated from the slope and ω_0 is derived by using the FT of $H(t)$. This method is useful for relatively low Q factors. However, for higher Q factors, the slope $\{\omega_0/(2Q)\}$ is very small which results in larger errors. The second method calculates both the energy losses radiated from an interface surrounding the cavity and the energy stored in the cavity. The Q factor is determined by substituting both values into Eq. (1). For the cavity modes of the analyzed structures, a little discrepancy between the two methods, proving the validity of the results based on these approaches.

In addition, the modal volume of the cavities can be estimated by inserting the calculated electric field distributions into the following equation:

$$V=[\{\varepsilon(\mathrm{r})|E(\mathrm{r})|2d3\mathrm{r}\}/\{\max[\varepsilon(\mathrm{r})|E(\mathrm{r})|3\}], \qquad (4)$$

where ε(r) is the dielectric constant, and E(r) is the electric field. The integration region in Eq. (4) is ±14a in the x-direction, 6√3a (=±12 rows) in the y-direction, and ±4.3a in the z-direction from the center of the cavity. It has been confirmed that the size of the region is sufficiently large for calculating Eq. (4). The electric field distribution (E_y) of the fundamental mode for a cavity without air hole displacement at both edges has been reproduced in the following graph:

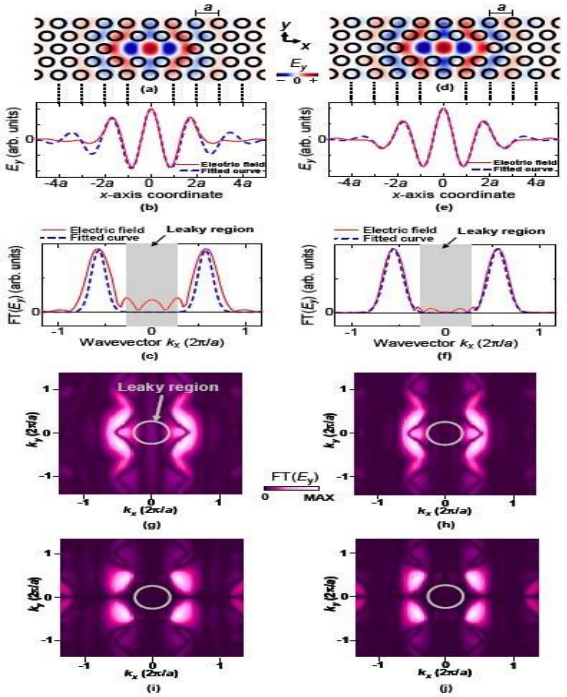

FIGURE 3. (a) The electric field distribution (E_y) of the fundamental mode for a cavity without air hole displacement at both edges. (b) The profile of (a) along the center line of the cavity and the fitted curve corresponding to the product of a fundamental sinusoidal wave and a Gaussian envelope function. (c) The 1D FT spectra of (b). The leaky region or light cone is indicated by the gray area. (d), (e), (f) The electric field distribution (E_y), the E_y profile at the center line and the fitted curve, and the 1D FT spectra, respectively, for the cavity structure shown in Fig.(3b). The

displacement of air holes at the edges is set at 0.20*a*. (g), (h). The 2D FT spectra of (a) and (d), respectively. (i), (j) The 2D FT spectra of E_x for cavities of (a) and (d), respectively. Figure courtesy Akahane Yoshihiro, Asano Takashi, Song Bong-Shik, and Noda Susumu, Fine-tuned high-Q photonic-crystal nanocavity, Optics Express, Vol. 13, Issue 4, pp.1202-1214 (2005), https://doi.org/10.1364/OPEX.13.001202.

Asano et al. (3) have studied Photonic crystal nanocavity with a Q factor exceeding eleven million, and presented their results of Decay curves of photons (Fig 4) in a nanocavity just after the fabrication (black solid line), after the first oxidization process (blue solid line), and after the subsequent oxide removal (DHF) process (red solid line). The cavity is excited by an input pulse with a width of 10 ns (gray dashed line). Their results have been reproduced below:

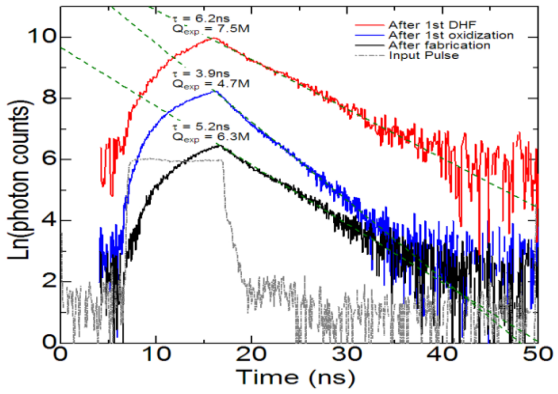

FIGURE 4. Decay curves of photons in a nanocavity just after the fabrication (black solid line), after the first oxidization process (blue solid line), and after the subsequent oxide removal (DHF) process (red solid line). The cavity is excited by an input pulse with a width of 10 ns (gray dashed line). The small dip at around 20 ns is attributed to the influence of the tail of the input pulse. We evaluated photon lifetimes (τ) from the later part (>25 ns) of the decay curves. Figure courtesy Akahane Yoshihiro, Asano Takashi ,Song Bong-Shik , and Noda Susumu, Fine-tuned high-Q photonic-crystal nanocavity, **Optics Express**, Vol. 13, Issue 4, pp. 1202-1214, (2005), Figure courtesy AsanoTakashi , Ochi Yoshiaki , Takahashi Yasushi , Kishimoto Katsuhiro, and Noda Susumu , Photonic crystal nanocavity with a *Q* factor exceeding eleven million, **Optics Express,** Vol. 25, Issue 3, pp. 1769-1777, (2017), https://doi.org/10.1364/OE.25.001769.

Figure 4 shows the photon lifetime curve of one of the prepared nanocavities just after fabrication, that after the first oxidization process and that after the first DHF process. It is seen in the figure that τ decreased from 5.2 ns to 3.9 ns after the oxidization and increased to 6.2 ns after the DHF treatment. The corresponding Q_{exp} values are 6.3, 4.7 and 7.5 million, respectively. Simultaneously, the resonant wavelength changed from 1567.5 nm to 1567.26 nm and 1565.30 nm for each treatment step. The blue shifts of the resonant wavelength are caused by the decrease of the refractive index by surface oxidization, and the decrease of the slab volume by oxide removal. The total blue shift of the resonant wavelength (2.2 nm) observed for this process corresponds to the uniform removal of silicon at the cavity surface (including inner walls of the air holes) by about 0.5 nm according to the 3D-FDTD calculation. The decrease of τ after the oxidization is due to the formation of interface states at the Si/SiO_2 interface, and the increase of τ after oxide removal is attributed to the removal of the interface states and termination of the Si surface with hydrogen. More importantly, one cycle of this treatment increased τ or Q_{exp} by 19%, which demonstrates the effectiveness of this cleaning method. Following the approach of Asano et al (3), $(1/Q_{imp})$ can be obtained from the statistical analysis of Q_{exp}. For this analysis, first step is to remove the loss determined by the design (Q_{des}) by using the following relation:

$$(1/Qexp) = \{1/Qdes+1/Qimp\}. \quad (5)$$

By using a Q_{des} value of 4×10^7, which is determined from the 3D-FDTD calculation including the load of the excitation waveguide; the evaluated average loss due to the imperfections [Avg.$(1/Q_{imp})$] and its standard deviation [S. D.$(1/Q_{imp})$] can be calculated. $(1/Q_{imp})$ can be divided into scattering loss $(1/Q_{scat})$ and absorption loss $(1/Q_{abs})$ as follows:

$$(1/Qimp) = \{1/Qscat+1/Qabs1\}. \quad (6)$$

$(1/Q_{scat})$ is mainly determined by the fluctuations of the structure, and $(1/_{Qabs})$ is determined by the light absorption of the material. The magnitude of $(1/Q_{scat})$ due to random air-hole variations can be calculated by using the FDTD simulations. In this calculation, random nanometer-scale variations in the positions and radii have to be applied to all the air holes in the calculation space in such a way that the probability of the variations followed a normal distribution with a standard deviation of σ_{hole}. This requires lot of expertise of the designer, and his knowledge of the subject. The calculation for different fluctuation patterns is done to obtain the statistical relationship between σ_{hole} (in nm) and Avg. $(1/Q_{scat})$ and σ_{hole} and S.D. $(1/Q_{scat})$ as follows:

$$\text{Avg. } (1/Qscat) = 7.5\times10\text{^ } (-7) \times (\ \sigma_{hole}\ \text{^2}), \quad (7)$$

and

$$\text{S.D. } (1/Qscat) = 3.0\times10\text{^ } (-7) \times (\ \sigma_{hole}\ \text{^2}\ ). \quad (8)$$

By assuming that the fluctuations of $(1/Q_{imp})$ are mostly determined by the variation of air holes and that the fluctuation of absorption loss can be ignored, i.e. S.D.$(1/Q_{imp})$ = S.D.$(1/Q_{scat})$, σ_{hole} is of the order of 0.24 ~0.26 nm . The designer has to design the mode volume and the quality factor of nanocavities, which are suitable for a particular application. Obviously, the lateral loss can be suppressed easily by increasing the number of photonic crystal layers around the cavity operating at the frequency inside the band gap. Therefore, the vertical loss mostly determines the total of the cavity. A single defect cavity formed by missing a hole in a square lattice, is known to support three types of defects modes: quadrupole, dipole, and monopole. The quadrupole mode has the highest quality factor with a, with 5 photonic crystal periods around the defect.

It has been established that small group velocity is very useful in many applications, like on-chip optical delay components, and the observation of non-linear phenomena at very low power levels. Besides, the reduced group velocity implies a larger density of photon states, which fact reduces the lasing threshold. Also, since the spatial modulation of the dielectric constant in photonic crystals is periodic, their dispersion behavior is different from that observed in case of uniform materials, as apart from the usual formation of bands and band gaps, it is also possible to obtain a large group velocity anomaly and a high density of optical states (DOS) at the band edges of bulk photonic crystals and of photonic crystal waveguides; though this anomaly is limited only to a very narrow range of wave vectors and for one particular direction of propagation.

Two-dimensional arrays of coupled photonic crystal nanocavities exhibiting flat band i.e. small group velocity or large optical density of states, in the whole range of wave vectors and in all crystal directions (4) have also been reported. Since there is a large group velocity anomaly in any photonic crystal direction, these arrays are able to give even higher output powers while preserving low lasing thresholds. Another advantage is that the electrical pumping in these structures is much easier. Also, these structures in combination with nonlinear optical materials can be used for exploring the 2D discrete solitons (5, 6), and constructing optical switching arrays. Interestingly, coupled resonator optical waveguides (CROWs) in photonic crystals have also been reported (7) as able to reduce the group velocity. In fact, a coupled-resonator optical waveguide simply consists of a chain of resonators in which light propagates by tunneling from one resonator to its adjacent resonators, and hence, the group velocity can be controlled by changing the distance between the resonators. An important factor to be taken care is that though the CROW is able to reduce the group velocity in a wide range of wave vectors, it has to be ensured that this propagates in the direction of the coupling of the cavities, which is quite difficult, and requires the skill of the designer, who has to align the input beam in one particular direction, and also to couple it efficiently into a cross sectional area.

The formation of the Localized Modes Induced by Structural Defects has been discussed by Dai (8). As explained in this paper, there are no propagating (real k) modes inside the band gap. However, for the case of the complex wave vector, H(x) is given by:

$$H(x) = e^{ikx}u(x) = e^{ik_0x}u(x)e^{-\kappa x}\,, \qquad (9)$$

which is decaying exponentially. The upper band near the gap can be approximated by expanding $\omega_2(k)$ in powers of k about the zone boundary $k = \pi/a$. Because of the time-reversal symmetry, the expansion cannot contain odd powers of k, and the following expression can be written:

$$\Delta\omega = \omega_2(k) - \omega_2(\pi/a) = \alpha(k - \pi/a)^2 = \alpha(\Delta k)^2\,. \qquad (10)$$

Hence, clearly for frequencies lower than the top of the gap, i.e., within the gap, $\Delta\omega < 0$, $\Delta k = i\kappa$ is purely imaginary. As the gap is traversed, the decay constant κ grows as the frequency reaches the mid-gap, then disappears at the gap edges, and subsequently disappears at the gap edges. In case of the perfect photonic crystals, because of the translational symmetry, the evanescent modes cannot be excited. Interestingly, however, a defect is able to sustain such a mode, because the corresponding translational symmetry is broke; and hence, a localized evanescent mode can be created within the photonic band gap. This concept is used for explaining the formation of photonic-crystal cavities and photonic-crystal waveguides. It has also been explained that by suitably perturbing the lattice sites, it can be assured that only a single mode or sets of closely spaced modes can be permitted that have frequencies in the gap. In addition, these modes have the characteristic of decaying exponentially away from the defect, and hence are confined. This explains the concept of photonic-crystal cavity based on photonic band gap confinement. The selected site may be perturbed, by various ways including (i) removing it from the crystal, and (ii) replacing it with another whose size or dielectric constant is different, Since the point defects in photonic crystal can be used to trap photons, the light can also be guided from one location to another by using line defects, i.e., by changing the dielectric constant along a line in a photonic crystal to generate modes lying within the band gap. In this way, lights of corresponding frequencies can be confined, and directed along the waveguide. Therefore, the $k = -\pi/a$ mode lies at an equivalent wave vector to the $k = \pi/a$ mode, and at the same frequency. So there is a degeneracy at the zone boundary, $k = \pi/a$. The E-fields can be expressed at the boundary as $e(x) = \cos(\pi x/a)$ and $o(x) = \sin(\pi x/a)$, a linear combination of $E(x) \sim e^{\pm kx}$, both at $\omega = c\pi/a$. ε can also be perturbed so that it is nontrivially periodic with periodicity a; for example, $\varepsilon(x) = 1\ \Delta\cos(2\pi x/a)$. It is important to note that the photonic crystals have also found application in the development of ring resonator. Gao et al (9) have proposed and demonstrated an air-mode photonic crystal ring resonator (PhCRR) on silicon-on-insulator platform. In this study, they have utilized the air mode to confine the optical field into photonic crystal (PhC) air holes, and have confirmed this by the three-dimensional finite-difference time-domain simulation. PhCRR structure has been employed to enhance the light-matter interaction by combining the whispering-gallery mode resonance of ring resonator with the slow-light effect in PhC waveguide. They have reported that in the simulated and measured transmission spectra of air-mode PhCRR, nonuniform in free spectral ranges (FSRs) are observed near the Brillouin zone edge of PhC, which indicates the presence of the slow-light effect. Also, they have experimentally obtained a maximum group index of 27.3, and a highest quality factor of 14600 near the band edge. It has been emphasized that benefiting from the strong optical confinement in the PhC holes and enhanced light-matter interaction in the resonator, the demonstrated air-mode PhCRR is expected to have potential applications in refractive index sensing, on-chip light emitting, and nonlinear optics by integration with functional materials, which shows their utility in research work. The proposed air-mode PhCRR, the geometrical parameters of the PhCRR structure, and the simulated resonant spectrum of the PhCRR

by 3D FDTD (9), have been reproduced in Fig.5 below:

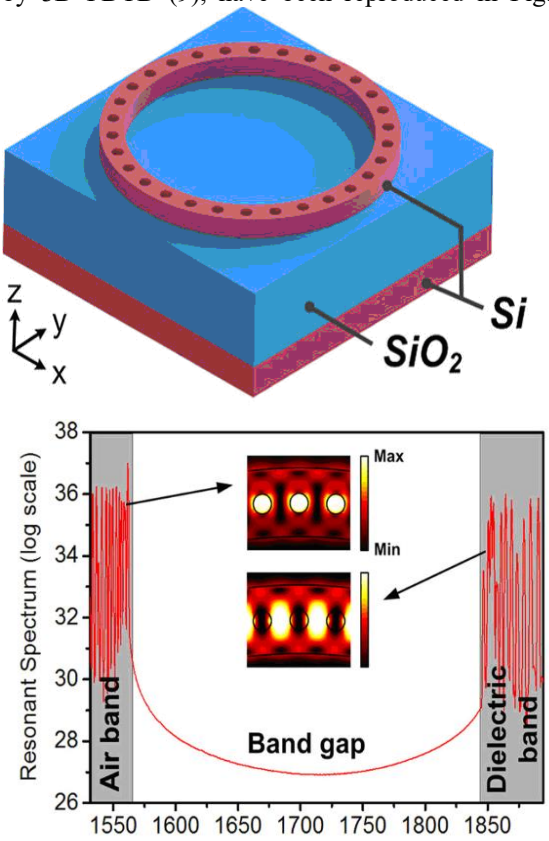

FIGURE 5. (Top) Proposed air-mode PhCRR; (Middle) Geometrical parameters of the PhCRR structure; and (Bottom) Simulated resonant spectrum of the PhCRR by 3D FDTD. Figure modified from the figure courtesy Gao et al Scientific Reports 6 (2016), Article number: 19999.

The simulated resonant spectrum of the air-mode PhCRR shows that (i) in 3D FDTD simulation, a TE-like polarized light excited by a dipole source in the ring resonator propagates through the PhCRR and then is monitored on the other side; and (ii) wavelength ranging from 1563 to 1845 nm corresponds to the photonic bandgap (PBG) region. It can also be noticed that (i) the resonant peaks on two sides of the PBG region are located in the air band and dielectric band, respectively; and (ii) close to the Brillouin zone edge, the resonant modes in the two bands both exhibit nonuniform free spectral ranges , indicating the presence of the slow-light effect. From the simulated band-edge resonant mode profiles shown in the insets , it can be seen that the optical field of the dielectric-band resonant mode is mainly localized in the dielectric region, while that of the air-band resonant mode has a good field overlapping with the PhC air holes.Faraon et al (10) have observed that Semiconductor quantum dots integrated in nano-cavities exhibit atom-like properties that can make them useful for the design of functional quantum information networks. Their Quantum network on a PC chip has been shown below:

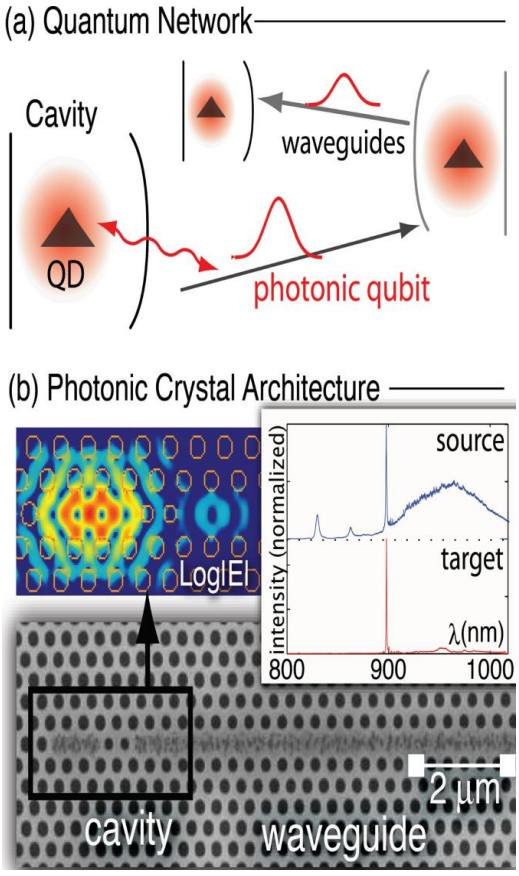

FIGURE 6. Quantum network on a PC chip. (a) Cavity-coupled quantum dots (QD) exchange qubits via waveguides. (b) Scanning electron micrograph of a PC structure combining cavities and waveguides. Insets: Electric field intensity and measured spectral filtering of cavity-waveguide-cavity structure. Figure courtesy Faraon Andrei, Englund Dirk, Fushman Ilya , and Vuckovic Jelena , Quantum information processing on photonic crystal chips, Conference on Quantum Optics, OSA Technical Digest (CD) (Optica Publishing Group, 2007), paper CMH3,15 April 2008.

IV. IMPORTANT EXPERIMENTAL BREAK-THROUGHS AND CONCLUDING REMARKS

An ultra-compact active hybrid plasmonic ring resonator has recently drawn interest for research work and device applications. Xiang et al (11) have designed an ultra-compact active hybrid plasmonic ring resonator for lasing applications at deep sub-wavelength scale, and have emphasized that the combined contributions of hybrid plasmonic mode, circular-shaped cross section of nanowire, and ring resonator structure with round-trip whispering-gallery cavity, result in reduced metallic absorption loss, tight mode confinement, and enhanced cavity feedback, and hence achieving high quality factor , small mode volume , high Purcell factor , low threshold gain , and ultra-small footprint with sub-micron size. Their results on the dependence of the Q factor and the mode volume (μ m^3) on the gap height for both HP and PH modes at a resonance in the lasing wavelength band have been reproduced below:

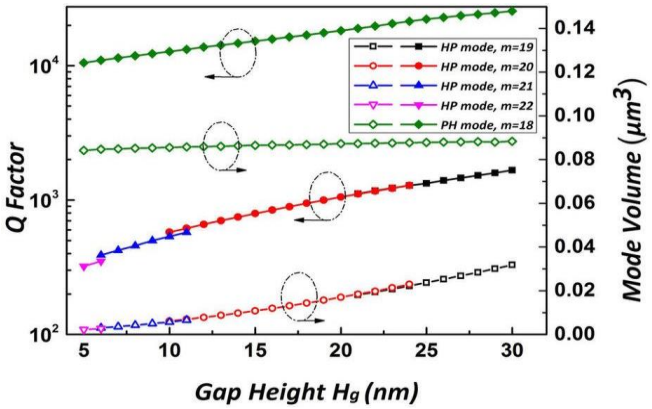

FIGURE7. Q factor and the mode volume (μ m^3) for both HP and PH modes at a resonance in the lasing wavelength band 100 nm, = 800 nm). Figure courtesy Xiang et al Scientific Reports 4 (2014), Article number: 3720.

This figure clearly shows the dependence of the new factor and the mode volume (μ m^3) on the gap height for both HP and PH modes at a resonance in the lasing wavelength band 100 nm to 800 nm). It is seen that with an increase of gap height from 5 to 30 nm, the factor increases from 300 to 1650 for the HP mode, due to less mode energy distributed in the silver substrate and the resultant low absorption loss. In case of the PH mode also, the factor increases as the gap height increases. Xiang et al. (11) have explained this phenomenon as: When the nanowire is lifted away from the metal substrate, less mode energy leaks into the metal substrate, which results in the reduction in the total loss of the resonator and the increase in the factor. Further, since the HP mode is tightly confined in the small gap region, the mode volume can be ultra-small (~ 0.0022) at sub-wavelength scale under a small a gap height of 5. The results show that (i) the mode volume changes from 0.0022 to 0.0318 as the gap height increases from 5 to 30 nm; and (ii) the mode volume of the PH mode, remains almost unchanged (0.0842–0.0884 μm^3), showing larger mode volume compared to the HP mode and less dependency of mode volume of the PH mode on the gap layer.

The importance of the photonic nanocavities has led to many recent experimental studies on the subject. Yaseen et al (12) have numerically and experimentally investigated the lateral coupling between photonic crystal (PhC) nanobeam (NB) cavities, pursuing high sensitivity and figure of merit (FOM) label-free biosensor. They have numerically carried out 3D finite-difference time-domain (3D-FDTD) and the finite element method (FEM) simulations, and have shown that when two PhC NB cavities separated by a small gap are evanescently coupled, the variation in the gap width significantly changes the coupling efficiency between the two coupled NB cavities, and the resulting resonant frequencies split. Also, they have fabricated laterally-coupled PhC NB cavities using (InGaAsP) layer on the InP substrate, and have shown that the laterally coupled PhC NB cavities sensor exhibits higher sensitivity than the single PhC NB cavity, which has been explained as due to the strong evanescent coupling between nearby PhC NB cavities, as it depends on the gap width, and is attributed to the large confinement of the electromagnetic field in the gap (air or liquid). In fact, the lateral coupling leads to the existence of both even (symmetric) and odd (asymmetric) modes. It has been shown that the even modes are more sensitive than odd modes. Therefore, the fabricated PhC NB cavity has been characterized and examined as a label-free biosensor, which is observed to exhibit high figure of merit due to its high -factor. This in fact, illustrates a potentially useful method for optical sensing at nanoscale.

Nakamura et al. (13) have presented a useful method for improving the quality factors of two-dimensional photonic crystal nanocavities using a three-dimensional finite-difference time domain calculation. It has been discussed that the leaky area for a high- nanocavity mode is visualized in a real cavity structure by extracting the leaky components within a light cone in momentum space and by transferring them back into real space using an inverse Fourier transformation. It has been emphasized that the factor is remarkably improved by appropriately shifting the positions of air holes at the leaky area. Nakamura et al. (13) have designed three-missing-air-hole and zero-cell-defect nanocavities with factors of 5,000,000 and 1,700,000, respectively, and also have demonstrated their performance. Ee et al. (14) have discussed that though the surface plasmon polariton modes often excited in metallic nanocavities enable the miniaturization of photonic devices, even beyond the diffraction limit, yet their severe optical losses deteriorate device performance; and have proposed a design of metallic nanorod cavities coupled to plasmonic crystals with the aim of reducing the radiation loss of surface plasmon modes. They have suggested that (i) the periodic Ag disks placed on an insulator–metal substrate open a substantial amount of plasmonic band gaps (e.g., =290nm at =1550nm) by modifying their diameter and thickness; (ii) when an Ag nanorod with a length of ~ 400nm is surrounded by the periodic Ag disks, its -factor increases up to 127, yielding a 16-fold enhancement compared with a bare Ag nanorod, while its mode volume can be as small; and (iii) Ag nanorods with gradually increasing lengths exhibit high -factor plasmonic modes that are tunable within the plasmonic bandgap. It has been emphasized that these numerical studies on low-radiation-loss plasmonic modes excited in metallic nanocavities are expected to promote the development of ultra small plasmonic devices.

Maeno et al. (15) have experimentally studied the photonic crystal L3 nanocavities whose design factors have been improved with the visualization of leaky components design method. It has been reported that the experimental values (Q_{exp}) are monotonically increased from 6,000 to 2,100,000 by iteratively modifying the positions of some of the air holes, as determined by the referred design method. In addition, the tolerance to imperfections in the fabricated samples has been investigated, which shows that the cavities improved by the visualization method tend to lose some tolerance to structural differences between the fabricated samples and the design values. These results are of tremendous importance in the research work using such nanocavities.

Another important study has been reported for the case of the high-quality Lithium niobate (LN) photonic crystal nanocavities. Liang et al. (16) have discussed that the Lithium niobate exhibits unique material characteristics, which have been found to be very useful indeed for many important applications. It has been explained that the scaling of LN devices down to a nanoscopic scale dramatically enhances the light–matter interaction, which in fact enables the nonlinear and quantum photonic functionalities, that is not possible by the conventional means. However, it is quite difficult to develop the LN-based nanophotonic devices, and so far, in spite of significant efforts made for the purpose; the researchers have met with only limited success, since the LN photonic crystal structures developed till recently had only low quality (Q). Liang et al. (16) have demonstrated LN photonic crystal nanobeam resonators with optical as high as 105105, which is more than two orders of magnitude higher than other LN photonic crystal nanocavities reported earlier. It has been emphasized that the high optical, together with tight mode confinement, leads to an extremely strong nonlinear photorefractive effect, with a resonance tuning rate of ~0.64 GHz/aJ or equivalently ~84MHz/photon, which is three orders of magnitude greater than other LN resonators. Interestingly, Liang et al. (16) have made the observation of an intriguing quenching of photo refraction, which has in fact been reported for the first time. An important conclusion of the study is that the demonstration of high- LN photonic crystal nanoresonators paves a crucial step toward LN nanophotonic, that could integrate the outstanding material properties with versatile nanoscale device engineering for diverse and intriguing functionalities; which will be extremely useful in future research and novel applications. Jannesari et al. (17) have presented a design for a high factor photonic crystal ring resonator (PCRR), based on 2D pillar type photonic crystals, which consist of a hexagonal array of silicon rods. The cavity has been created by removing elements from the regular PhC grid. It has been emphasized that the advantage of this PCRR is that it is possible to achieve strong confinement of light intensity in the low index region (filled with the gaseous analyte), and hence the interaction of light and analyte, which can be a liquid or a gas, is enhanced, due to the high quality factor of the cavity ($=1.2\times10^4$), along with strong overlap between the field of the resonant mode and the analyte, as well as the low group velocity of PCRR modes. It has been suggested that an enhancement factor of 1.149×10^5 compared to the bulk light absorption in a homogenous material provides the potential for highly sensitive gas detection with a photonic crystal ring. Witmer et al (18) have discussed that (i) the future quantum networks, in which superconducting quantum processors are connected via optical links will require microwave-to-optical photon converters that preserve entanglement; and (ii) a doubly-resonant electro-optic modulator (EOM) is a promising platform to realize this conversion. Witmer et al (15) have presented their progress towards building such a modulator by demonstrating the optically-resonant half of the device, and have demonstrated high quality (Q) factor ring, disk and photonic crystal resonators using a hybrid silicon-on-lithium-niobate material system. It has been stated that the Optical factors up to 730,000 have been achieved, corresponding to propagation loss of 0.8 dB/cm. Witmer et al (18) have also used the electro-optic effect to modulate the resonance frequency of a photonic crystal cavity, which is able to achieve electro-optic modulation coefficient between 1 and 2pm/V. It has been emphasized that in addition to quantum technology, these results are expected to be useful both in traditional silicon photonics applications and in high-sensitivity acousto-optic devices.

Lee et al. (19) have studied Deterministic coupling of delta-doped NV centers to a nanobeam photonic crystal cavity. As emphasized by them, the negatively charged nitrogen vacancy center (NV) in diamond has generated significant interest as a platform for quantum information processing and sensing in the solid state. Since, for most applications, high quality optical cavities are required to enhance the NV zero-phonon line (ZPL) emission. An outstanding challenge in maximizing the degree of NV-cavity coupling is the deterministic placement of NVs within the cavity, they have reported photonic crystal nanobeam cavities coupled to NVs incorporated by a delta-doping technique that allows nanometer-scale vertical positioning of the emitters. In addition, they have demonstrated cavities with Q up to ~24 000 and mode volume $V \sim 0.47(\lambda/n)^3$ as well as resonant enhancement of the ZPL of an NV ensemble with Purcell factor of ~20. They have claimed that their fabrication technique provides a first step towards deterministic NV-cavity coupling using spatial control of the emitters. The Resonant enhancement and lifetime reduction of NV ZPL. (a) A two-dimensional intensity plot (log scale) of the PL spectrum at different cavity tuning steps has been reproduced below:

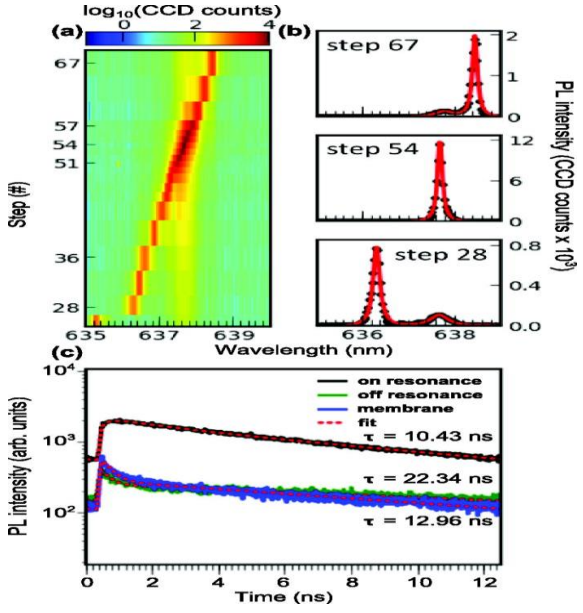

FIGURE 8. Resonant enhancement and lifetime reduction of NV ZPL. (a) A two-dimensional intensity plot (log scale) of the measurements e PL spectrum at different cavity tuning steps. (b) PL spectrum when the cavity mode is off-resonance, on-resonance, and then off-resonance. The cavity mode starts at a wavelength shorter than the NV ZPL (step 28).

The intensity of the NV ZPL is enhanced by ∼40 times when the cavity mode is tuned on resonance. The NV ZPL intensity then decreases as the cavity mode is tuned off-resonance. (c) Lifetime of NV centers are performed when the cavity mode is off resonance (green curve), and on resonance (black curve). NV lifetime is also measured from an un-patterned membrane (blue curve). Lifetime reduction is observed when the NV center is on-resonance with the cavity mode. The lifetime curves are best fit with a double exponential decay (red dotted curve). Figure courtesy Lee Jonathan C, Bracher David, Cui Shanying, McLellan ClaireA., Zhang Xingyu, Andrich Paolo; Alemán Benjamin, Russell Kasey J., Magyar Igor Aharonovich, Bleszynski JayichAnia, Awschalom David , Hu Evelyn L, and Ohno Kenichi, Deterministic coupling of delta-doped NV centers to a nanobeam photonic crystal cavity, Appl. Phys. Lett. **105**, 261101 (2014) https://doi.org/10.1063/1.4904909.

As in case of Optical technology, which has seen a revival from the previous decade, in terms of innovations and research, especially relating to optical integrated circuits, Photonic Crystals (PCs) are one of the main contenders for the purpose. Therefore, the research work of Rehman et al. (20) implicates different arrangements of the 3-Dimensional PC units based on the employment of a varying radius PC-cavity and its position i.e., at the beginning and within the middle of the PC-lattice. Researchers have recently focused on studying the effects of these PC-cavities, investigating higher shifting in resonant wavelength, a narrower line width around 0.0061 μm and a quality factor of 99.59, comprising of a PC-cavity of radius 0.300 μm using input signal only i.e., coupled into the optical structure using the phenomenon of the Guided-mode-resonances (GMR). They have computed the structures by using an open-source FDTD platform, employing a stripe-model-based structure utilizing the Periodic Boundary Condition to save time and computational resources and later the PML for the realization of the Finite models. Most importantly, they have demonstrated the concluded structures based on the position of the PC-cavity, for the design of the all-optical-amplification device, executing a control signal reporting an 8 % of the amplification in the output of the input signal. This result is of tremendous utility in the research and development work regarding Photonic crystals. Their results of arrangements based on the sum of the PC-units have been reproduced below:

A comparative study of the photonic crystals-based cavities and usage in all-optical-amplification phenomenon, Photonics and Nanostructures Fundamentals and Applications, Volume 61, September 2024, 101298, Ali et al. (21) have Illustrated the potential of the novel concepts by fabricating nanostructures that are impossible to make with any other known method: waveguide-coupled high-Q silicon photonic cavities that confine telecom photons to 2 nm air gaps with an aspect ratio of 100, corresponding to mode volumes more than 100 times below the diffraction limit. Scanning transmission electron microscopy measurements confirm the ability to build devices with sub-nanometre dimensions. Our work constitutes the first steps towards a new generation of fabrication technology that combines the atomic dimensions enabled by self-assembly with the scalability of planar semiconductors.

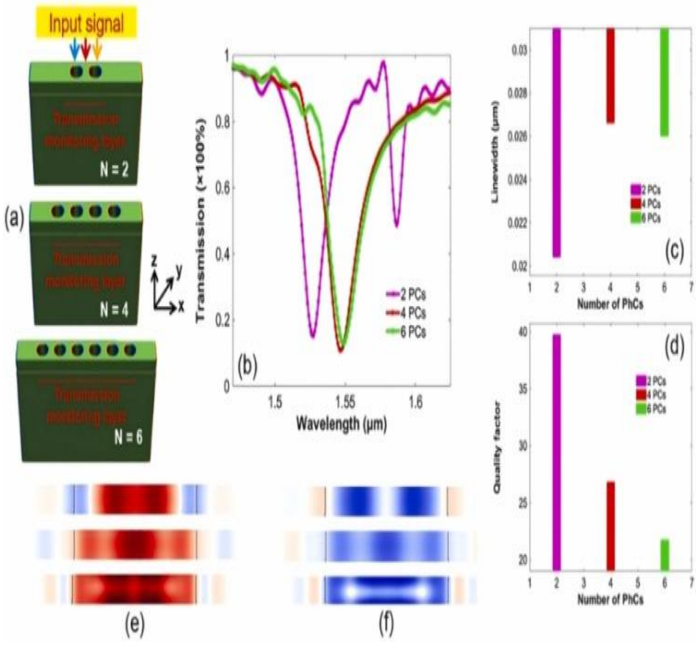

FIGURE 9. (a) Arrangements based on the sum of the PC-units i.e., 2, 4 and 6 (b) Output transmission spectra of the structures comprising of 2, 4 and 6 PC-units (c) Linewidth of the 2, 4 and 6 PC-units (d) Quality factor-based on the sum of the PC-units i.e., 2, 4 and 6 (e) Electric field confinement by 2, 4 and 6 PC-units (f) Magnetic field onfinement by 2, 4 and 6 PC-units, respectively. Figure courtesy Rehman Atiqur, Khan Yousuf, Ahmad Umair, Muhammad Irfan, Muhammad Rizwan Amirzada , and Muhammad Ali Butt,

A comparative study of the photonic crystals-based cavities and usage in all-optical-amplification phenomenon, Photonics and Nanostructures Fundamentals and Applications, Volume 61, September 2024, 101298, Ali et al. (21) have Illustrated the potential of the novel concepts by fabricating nanostructures that are impossible to make with any other known method: waveguide-coupled high-Q silicon photonic cavities that confine telecom photons to 2 nm air gaps with an aspect ratio of 100, corresponding to mode volumes more than 100 times below the diffraction limit. Scanning transmission electron microscopy measurements confirm the ability to build devices with sub-nanometre dimensions. Our work constitutes the first steps towards a new generation of fabrication technology that combines the atomic dimensions enabled by self-assembly with the scalability of planar semiconductors.

Maine et al. (22) have discussed in detail Optically triggered Q-switched photonic crystal laser The results **of** Photonic crystal cavity modes and simulated Qs, as given in the literature have been reproduced below:

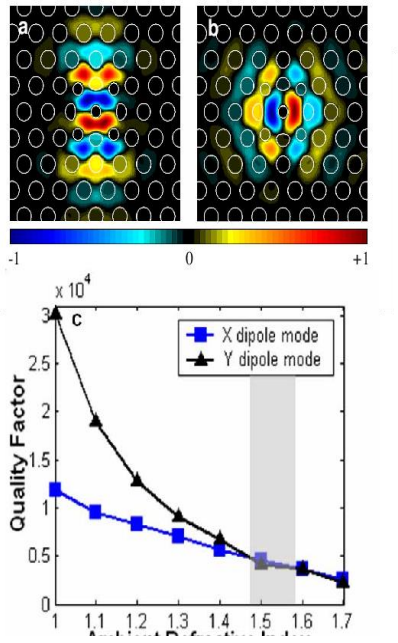

FIGURE 10. Photonic crystal cavity modes and simulated Qs. Finite-difference time-domain simulation of Z component of magnetic field for a, X-polarized and b, Y-polarized modes c, Simulated Q for X and Y-polarized cavity modes as a function of the ambient refractive index. Although the X-polarized mode has a Q significantly below that of the Y-polarized mode in air, both possess comparable Qs above 4000 even at an ambient refractive index of n ~ 1.5. Shaded region denotes ambient refractive index accessible by the infiltrated LC. Figure modified from the Figure courtesy researchgate.net.

13th International Conference (23) on Metamaterials, Photonic Crystals and Plasmonics, Paris, France was held recently, where the novel concepts and applications of nanomaterials were discussed. The fields of Metamaterials (engineered materials that have properties not found in naturally occurring materials, "meta" in Greek meaning "beyond") and Plasmonics. Nanophotonics (optical interactions with nanostructures and nanomaterials) have opened new opportunities for controlling electromagnetic waves in the sub-wavelength regime. Study and application of these interactions involve various scientific disciplines, i.e. engineering, physics, chemistry, material science, biology, medicine, information technology, energy, and communications. 14th International Conference (24) on Metamaterials, Photonic Crystals and Plasmonics was held in Toyama, Japan. Another International Conference (25) on Nanoscience, Nanotechnology and Advanced Materials (IC2NM-2024) is going to be held in Brisbane, Australia. Thus, it can be concluded that the subject of nanotechnology is evolving very rapidly for novel applications and research work.

ACKNOWLEDGEMENTS

The authors are grateful to Dr. Nand Kishore Garg, Founder Chairman, Maharaja Agrasen Institute of Technology, GGSIP University, Delhi for providing the facilities for carrying out this research work, and also for his moral support. The authors are thankful to Dr. M. L. Goyal, Vice Chairman (Academic) and Dr. Satvir Singh Deswal, Dean (Academic) for encouragement. The authors are also thankful to the listed researchers and agencies for providing the images.

REFERENCES

[1] Ryu, H.-Y., Notomi, M. and Lee, Y.-H., *High-quality-factor and small-mode-volume hexapole modes in photonic-crystal-slab nanocavities*, Appl. Phys. Lett.**83**, 4294 (2003).
[2] Akahane, Y., Asano, T., Song, B.-S. and Noda, S., *Fine-tuned high-Q photonic-crystal nanocavity, Optics* Express **13**, 1202-1214 (2005), https://doi.org/10.1364/OPEX.13.001202.
[3]Asano, T., Ochi, Y., Takahashi, Y., Kishimoto Katsuhiro, and Noda Susumu , *Photonic crystal nanocavity with a Q factor exceeding eleven million, Optics* Express **25**, 1769-1777 (2017), https://doi.org/10.1364/OE.25.001769.
[4] Altug, H. and Vuckovic, J., *Two-dimensional coupled photonic crystal resonator arrays*, Appl.Phys. Lett. **84**, 161-163 (2004).
[5] Fleischer, J. W., Segev, M., Efremidis, N. K. and Christodoulides, D. N., *Observation of two-dimensional discrete solitons in optically induced nonlinear photonic lattices*, *Nature (London)* **422**, 147–150 (2003).
[6] Christodoulides, D. N. and Efremidis, N. K., *Discrete temporal solitons along a chain of nonlinear coupled microcavities embedded in photonic crystals*, Opt. Lett. **2**, 568-570 (2002).
[7] Yariv, A., Xu, Y., Lee, R. K. and Scherer, A., *Coupled-resonator optical waveguide: a proposal and analysis, Optics* Lett. **24**, 711 (1999).
[8] Dai, B., *Manipulating Light with Photonic Crystal*, May 21, 2008; (Submitted as coursework for Applied Physics **273**, Stanford University, Spring, 2007); http://large.stanford.edu/courses/2007/ap273/dai1/.
[9] Gao, G., Zhang, Y., Zhang, H., Wang, Y., Huang, Q. and Xia, J., *Air-mode photonic crystal ring resonator on silicon-on-insulator*, Scientific Reports **6**, 19999 (2016).
[10] Faraon, A., Englund, D., Fushman, I. and Vuckovic, J.,*Quantum information processing on photonic crystal chips, Conference on Coherence and Quantum Optics, OSA Technical Digest (CD)* (Optica Publishing Group, 2007), paper CMH3,**15** April (2008).
[11] Xiang, Ch., Chan, Ch.-K., and Wang, J., Proposal and numerical study of ultra-compact active hybrid plasmonic resonator for sub-wavelength lasing applications , Scientific Reports **4**, 3720 (2014).
[12] Yaseen, M. T., Yang, Y.-Ch., Shih, M.-H. and Chang, Y.-Ch., *Optimization of High-Q Coupled Nanobeam Cavity for Label-Free Sensing*, Sensors **15**, 25868-25881 (2015).

[13] Nakamura, T., Takahashi, Y., Tanaka, Y., Asano, T. and Noda, S., *Improvement in the quality factors for photonic crystal nanocavities via visualization of the leaky components*, Optics Express **24**, 9541-9549 (2016).

[14] Ee, H.-S., Park, H.-G. and Kim, S.-K., *Design of high Q-factor metallic nanocavities using plasmonic bandgaps*, Applied Optics **55,** 1029-1033 (2016).

[15] Maeno, K., Takahashi, Y., Nakamura, T., Asano, T. and Noda, S., *Analysis of high-Q photonic crystal L3 nanocavities designed by visualization of the leaky components Optics* Express **25**, 367-376 (2017).

[16] Liang, H., L., R., He, Y., Jiang, H. and Lin, Q., *High-quality lithium niobate photonic crystal nanocavities, Optica* **4**, 1251-1258 (2017).

[17] Jannesari, R., Grille, T. and Jakoby, B., *Gas sensing with a high-quality-factor photonic crystal ring resonator*, *Proceedings* Volume **10242**, Integrated Optics: Physics and Simulations III; 1024205 (2017); Event: SPIE Optics + Optoelectronics, 2017.

[18] Witmer, J. D., Valery, J. A., Arrangoiz-Arriola, P., Sarabalis, Ch. J., Hill, J. T. and Safavi-Naeini, A. H., *High-Q photonic resonators and electro-optic coupling using silicon-on-lithium-niobate*, Scientific Reports **PMC5390248**; Sci Rep. **7**, 46313 (2017).

[19] Lee, J. C, Bracher, D., Cui, Sh., McLellan, C. A., Zhang, X., Andrich, P., Alemán, B., Russell, K. J., Magyar, I., Aharonovich, B. J., Awschalom, D., Hu, E., L. and Ohno, K., *Deterministic coupling of delta-doped NV centers to a nanobeam photonic crystal cavity*, Appl. Phys. Lett. **105**, 261101 (2014) https://doi.org/10.1063/1.4904909.

[20] Rehman, A., Khan, Y., Ahmad, U., Muhammad, I., Muhammad, R. A. and Muhammad, A. B., *A comparative study of the photonic crystals-based cavities and usage in all-optical-amplification phenomenon, Photonics and Nanostructures - Fundamentals and Applications* **61**, 101298 (2024).

[21] Ali, N. B., Thor, A. S. W., Konstantinos, T., Shima, K., Guillermo, A. , Babak, V. L. and Søren, S., *Self-assembled photonic cavities with atomic-scale confinement*, *Nature* **624**, 57–63 (2023).

[22] Maune, B., Witzens, J., Baehr-Jones, T., Kolodrubetz, M., O*ptically triggered Q-switched photonic crystal laser*, *Optics Express* **13**, 4699-707 (2015), DOI:10.1364/OPEX.13.004699.

[**23**] META 2023, *13th International Conference on Metamaterials, Photonic Crystals and Plasmonics*, Paris, France, July 18 – 21, 2023.META 2023.

[24] *14th International Conference on Metamaterials, Photonic Crystals and Plasmonics*, Toyama, Japan, July 16 – 19 (2024).

[25] *International Conference on Nanoscience, Nanotechnology and Advanced Materials* (IC2NM-2024), 8th Oct 2024 Brisbane, Australia (2024).